Dynamical fermion mass generation and exciton spectra in graphene

Chun-Xu Zhang,[1,2,*] Guo-Zhu Liu,[3,4,†] and Ming-Qiu Huang[1,‡]

[1]*Department of Physics, National University of Defense Technology, Changsha, Hunan 410073, People's Republic of China*
[2]*Interdisciplinary Center for Theoretical Study, University of Science and Technology of China, Hefei,*
Anhui 230026, People's Republic of China
[3]*Department of Modern Physics, University of Science and Technology of China, Hefei, Anhui 230026, People's Republic of China*
[4]*Institut für Theoretische Physik, Freie Universität Berlin, Arnimallee 14, D-14195 Berlin, Germany*

The Coulomb interaction between massless Dirac fermions may induce dynamical chiral symmetry breaking by forming excitonic pairs in clean graphene, leading to semimetal-insulator transition. If the Dirac fermions have zero bare mass, an exact continuous chiral symmetry is dynamically broken and thus there are massless Goldstone excitons. If the Dirac fermions have a small bare mass, an approximate continuous chiral symmetry is dynamically broken and the resultant Goldstone-type excitons become massive, which is analogous to what happens in QCD. In this paper, after solving the Dyson-Schwinger gap equation in the presence of a small bare fermion mass, we found a remarkable reduction of the critical Coulomb interaction strength for excitonic pair formation and a strong enhancement of dynamical fermion mass. We then calculate the masses of Goldstone-type excitons using the Shifman-Vainshtein-Zakharov sum-rule method and operator product expansion technique developed in QCD and find that the exciton masses are much larger than bare fermion mass but smaller than the width of dynamical fermion mass gap. We also study the spin susceptibilities and estimate the masses of non-Goldstone-type excitons using the same tools.

PACS number(s): 71.10.Hf, 71.30.+h, 73.20.Mf, 11.30.Rd

I. INTRODUCTION

Graphene is a recently fabricated two-dimensional electron system. It has attracted a great deal of research activities since it exhibits many interesting properties and also has remarkable potential technical applications.[1,2] Its fundamental low-energy degrees of freedom are two-dimensional massless Dirac fermions, which obey the relativistic Dirac equation. Due to the special linear dispersion of Dirac fermions, the density of states vanishes linearly near the touching points of conduction and valence bands. Therefore graphene is classified as a semimetal and the Coulomb interaction between massless Dirac fermions is unscreened.

The semimetal ground state of graphene is stable when the Coulomb interaction is weak. Its microscopic action respects an exact continuous chiral symmetry. Due to the masslessness of Dirac fermions, the graphene exhibits highly unusual behaviors, such as minimum conductivity,[1,2] quantum Hall effect,[3] and marginal Fermi-liquid behavior,[4] However, when the Coulomb interaction is sufficiently strong, a finite mass gap will be dynamically generated due to excitonic pairing instability.[5–12] As a consequence, the continuous chiral symmetry is broken and the graphene undergoes a quantum phase transition from semimetal to excitonic insulator. The mechanism underlying this phase transition can be considered as a concrete realization of the nonperturbative phenomenon of dynamical chiral symmetry breaking (DCSB) that was originally proposed by Nambu and Jona-Lasinio in the context of particle physics.[13]

Once a finite fermion mass is generated dynamically, both the ground state and the low-energy elementary excitations of graphene are fundamentally changed. The ground state becomes insulating, and the only low-energy excitations are massless Goldstone bosons induced by dynamical breaking of exact continuous chiral symmetry. These bosons are composed of quasiparticles (fermion) and quasiholes (antifermion), called excitons, and dominate the low-energy behaviors of graphene.

Note that the excitonic pairing triggered by Coulomb interaction is not the only way to generate a fermion mass gap. For example, the Kekule-type distortion can open a small fermion gap.[14–16] Moreover, the spin-orbit interaction may generate a small fermion gap that has opposite sign at K and K' points,[17] which was proposed to be able to turn graphene into a topological insulator.[17] Other gap generating mechanisms (for instance, geometry confinement) are also possible.[18] From an experimental point of view, a finite fermion mass gap is expected to be present if there is an exponential suppression of certain observable quantities, such as specific heat and susceptibility, at low temperature. However, the graphene may display different behaviors if the fermion gap is generated by different mechanisms. To see this clearly, it is helpful to make a symmetry analysis since different gap generating mechanisms are usually associated with different symmetry-breaking patterns.

When there is no excitonic pairing instability, the fermion mass may be generated by other mechanisms such as Kekule distortion. In this case, the continuous chiral symmetry is broken explicitly, rather than dynamically, and there are no Goldstone-type excitons. If the fermion mass is completely generated by excitonic pairing instability, then there are massless Goldstone-type excitons. The third possibility is that more than one mechanism is important. Before the Coulomb interaction is turned on, the Dirac fermions may already have a finite mass due to a certain mechanism. If this bare mass is small, the system possesses an approximate continuous chiral symmetry. When the Coulomb interaction is turned on, the Dirac fermions can acquire further mass gap due to excitonic pair formation. Once this happens, the approximate continuous

chiral symmetry is dynamically broken.[19] As a consequence, the Goldstone-type excitons have finite masses.[19]

We believe that the third possibility is of particular interest for two reasons. First, this possibility can happen in realistic graphene materials. For instance, when Coulomb interaction and Kekule distortion (or other mechanisms that can induce bare fermion mass) are both present, there may be dynamical breaking of approximate chiral symmetry. Second, the physical picture of this possibility is very similar to what happens in QCD. In QCD, it is well known that the *u* and *d* quarks have small bare masses. When these quarks acquire dynamical mass due to the formation of chiral condensate, the approximate chiral symmetry is dynamically broken and there appear massive Goldstone bosons, which are identified as the π mesons.[19] The massive Goldstone-type excitons generated in graphene correspond to the massive π mesons in QCD.

In this paper, we study the dynamical breaking of approximate chiral symmetry in graphene. We first assume a bare constant mass for the Dirac fermions, and then calculate the dynamical fermion mass by solving the corresponding Dyson-Schwinger (DS) gap equation. From the solutions, the chiral condensate can be easily obtained. We will show that a small bare fermion mass can greatly catalyze the formation of excitonic pairs. The critical Coulomb interaction strength for excitonic pairing instability is reduced to zero, while the dynamical fermion gap is significantly enhanced.

The dynamical fermion gap breaks the approximate chiral symmetry, so there appear massive Goldstone-type excitons. Now a natural problem is to estimate the masses of these excitons, which can help us to understand the low-energy excitations in the dynamical symmetry-breaking phase. The close analogy between the approximate DCSB behaviors in graphene and in QCD allows us to calculate the exciton mass using the tools developed in QCD. In particular, we will use the Shifman-Vainshtein-Zakharov (SVZ) sum-rule method and the operator product expansion (OPE) technique. OPE was proposed independently by Wilson[20] and by Kadanoff.[21] Wilson's motivation came from the urgency to study the problem of strong interactions associated with the nuclear force, while Kadanoff applied the OPE to understand critical phenomena in condensed-matter physics. Nowadays, OPE is known to be a powerful tool of quantum field theory describing elementary particle physics[22] and condensed-matter physics.[23] The SVZ sum rule technique was developed with the aim to understand strong interaction.[24,25] Among its wide applications in hadronic physics, the SVZ sum rule is particularly powerful in calculating the masses of mesons and baryons that are bound states of quarks and/or antiquarks. These methods were also applied to condensed-matter systems, including degenerate electron gas[26] and the cold atom system.[27] In this paper, we calculate the masses of excitons using these analytical tools.

These Goldstone-type excitons are associated with the onset of charge-density wave (CDW) or spin-density wave (SDW) orders. In addition to these excitations, there are also collective spin triplet excitons, which are not related to any symmetry breaking. The masses of these non-Goldstone-type excitons will also be calculated by means of the same SVZ sum-rule and OPE methods. We hope these exciton modes could be found

in future experiments (such as inelastic neutron scattering) in clean graphene sheet.

The rest of this paper is organized as follows. In Sec. II, we give the continuum model of two-dimensional Dirac fermions interacting through Coulomb potential. We study the DS gap equation in the presence of small bare fermion mass and calculate the chiral condensate using the dynamical fermion mass. In Sec. III, we study the Goldstone-type excitons and calculate their masses using the SVZ sum-rule and OPE techniques. In Sec. IV, the masses of non-Goldstone-type spin excitons are calculated. We give a brief summary and conclusion in Sec.V.

II. DYSON-SCHWINGER EQUATION AND DYNAMICAL MASS GENERATION

Since the seminal work of Nambu and Jona-Lasinio, DCSB has been investigated in the context of particle physics for nearly 50 years.[13,28–33] In particular, it is one of the most prominent features of QCD. Unfortunately, the structure of QCD is too complicated, so the problem of DCSB in QCD has not yet been solved satisfactorily, although there has been remarkable progress in its supersymmetric version.[34]

In order to gain insights into QCD, some theorists turn to QED_3. Despite its simple structure, QED_3 shares a number of salient features with QCD: asymptotic freedom,[35] DCSB,[32] and confinement.[36,37] Specifically, Appelquist *et al.* found that DCSB can take place when the fermion flavor is less than certain critical value, $N_f < N_f^c$ in QED_3.[32] Besides its relevance to particle physics, QED_3 of massless Dirac fermions also has important applications in condensed-matter physics. Indeed, it is the low-energy effective-field theory for a wide class of planar strongly correlated electron systems, especially high-temperature cuprate superconductors.[38] The DCSB in QED_3 is interpreted as the formation of two-dimensional Heisenberg antiferromagnetic order, which is the ground state of undoped cuprates.[38]

In the case of graphene, the Coulomb interaction between Dirac fermions plays an essential role since it is poorly screened. There is a close similarity between the low-energy continuum theory of graphene and QED_3. It is therefore not surprising that Coulomb interaction can lead to DCSB. However, there is also an important difference: the Coulomb potential is nonrelativistic and contains only the temporal component of the gauge field. Furthermore, although the massless Dirac fermions are two dimensional, the electromagnetic field propagates in three spatial dimensions.

Following Ref. 6, we describe the Dirac fermions in graphene by reducing QED_4 to $(2 + 1)$ dimensions. The effective action has the form

$$
\begin{aligned}
S = \int dt d^2r \, \bar{\psi}_s(t,\mathbf{r})(i\gamma^0\partial_t - iv_F\gamma^i\partial_i - m_s)\psi_s(t,\mathbf{r}) \\
- \frac{1}{2}\int dt dt' d^2r d^2r' \, \bar{\psi}_s(t,\mathbf{r})\gamma^0\psi_s(t,\mathbf{r})U_0(t-t',|\mathbf{r}-\mathbf{r}'|) \\
\times \bar{\psi}_{s'}(t',\mathbf{r}')\gamma^0\psi_{s'}(t',\mathbf{r}'),
\end{aligned}
\tag{1}
$$

where the Fermi velocity $v_F = c/300$ and subscripts s, $s' = 1,2$(or $\uparrow$, $\downarrow$) are the spin indices. The spinor field is

$\psi = (A_K, B_K, B_{K'}, A_{K'})$ with sublattice indices A, B and momentum valley indices K, K'. The γ matrices are defined as

$$\gamma_0 = \begin{pmatrix} 0 & 1_2 \\ 1_2 & 0 \end{pmatrix}, \quad \gamma_i = \begin{pmatrix} 0 & -\sigma_i \\ \sigma_i & 0 \end{pmatrix},$$

$$\gamma_3 = \begin{pmatrix} 0 & -\sigma_3 \\ \sigma_3 & 0 \end{pmatrix}, \quad \gamma_5 = \begin{pmatrix} 1_2 & 0 \\ 0 & -1_2 \end{pmatrix},$$

which are used by Refs. 3 and 39, and obey the Clifford algebra $\{\gamma_\mu, \gamma_\nu\} = 2g_{\mu\nu}$ with $\mu, \nu = 0, 1, 2$. Both γ_3 and γ_5 anticommute with γ_μ. Note that different choices of the γ matrices do not change the final results obtained in this section. The bare Coulomb potential $U_0(t, r)$ between Dirac fermions is given by

$$U_0(t, r) = \frac{e^2 \delta(t)}{\epsilon r}, \tag{2}$$

where ϵ is the dielectric constant. In graphene, it is convenient to define a fine structure constant as $\alpha = e^2/\epsilon \hbar v_F$. It takes different values when graphene is placed on different substrates. For graphene on substrate SiO_2, $\alpha \approx 0.8$; for graphene in vacuum (suspended), $\alpha = 2.2$.[12,18]

When the Dirac fermions are massless, $m_s = 0$, the Lagrangian (1) has an exact continuous chiral symmetry, $\psi \to e^{i\theta \gamma_{3,5}} \psi$. However, this symmetry is not respected by the mass term $\bar{\psi}\psi$. Besides, when a finite fermion mass is generated by formation of excitonic pairs due to Coulomb interaction, this symmetry will be dynamically broken. Using the DS equation approach, it is argued that a sufficiently strong long-range Coulomb interaction can induce a dynamical fermion mass, $\langle \bar{\psi}\psi \rangle \neq 0$, thus leading to quantum phase transition from semimetal to excitonic insulator.[5–7,11]

When the Dirac fermions have a small bare mass m_s with $s = 1, 2$, the Lagrangian respects only an approximate chiral symmetry. We will solve the corresponding gap equation in the presence of a small bare fermion mass and calculate the vacuum chiral condensate $\langle \text{vac}|\bar{\psi}_s \psi_{s'}|\text{vac}\rangle$, which is essential for the later computation of exciton mass in the next section. Due to the above definition of gamma matrices, the mass term $\bar{\psi}\psi$ corresponds to Kekule distortion.[3,16] More generally, Kekule distortion is formulated by $(\text{Re}\delta)\bar{\psi}\psi + (\text{Im}\delta)\bar{\psi} i\gamma_5 \psi$,[3] but it can be transformed into $m\bar{\psi}\psi$ with $m = \sqrt{(\text{Re}\delta)^2 + (\text{Im}\delta)^2} = |\delta|$ by absorbing the phase into the 4-spinor ψ.[15] We should also note that the physical origin of bare mass does not affect the solution of the gap equation and the magnitude of the corresponding mass generation only depends on the magnitude of the bare mass. For simplicity, we are mainly interested in the case where m_1 and m_2 are nearly the same, i.e., $|m_1 - m_2| \ll m$ with $m = (m_1 + m_2)/2$.

The DS equation for the Dirac fermion propagator of ψ_1 reads[11]

$$S^{-1}(p_0, \mathbf{p}) = S_0^{-1}(p_0, \mathbf{p}) - ie^2 \int \frac{dk_0}{(2\pi)} \frac{d^2k}{(2\pi)^2} V(p_0 - k_0, \mathbf{p} - \mathbf{k})$$
$$\times \gamma^0 S(k_0, \mathbf{k}) \gamma^0, \tag{3}$$

where the bare propagator is

$$S_0(p_0, \mathbf{p}) = \frac{1}{p_0 \gamma^0 - \mathbf{p}\gamma - m_1}, \tag{4}$$

and the full fermion propagator has the form

$$S(p_0, \mathbf{p}) = \frac{1}{p_0 \gamma^0 - \mathbf{p}\gamma - \Delta_1(p_0, \mathbf{p})}. \tag{5}$$

Hereafter we use the unit $v_F = 1$. Following previous works,[5,6] we adopt the instantaneous approximation and replace the gap function $\Delta_1(p_0, \mathbf{p})$ by $\Delta_1(0, \mathbf{p})$. Then we have

$$\Delta_1(\mathbf{p}) = m_1 + \frac{\alpha}{2} \int \frac{d^2k}{2\pi} J(\mathbf{p}, \mathbf{k}) \frac{\Delta_1(\mathbf{k})}{\sqrt{\mathbf{k}^2 + \Delta_1(\mathbf{k})^2}} \tag{6}$$

with the kernel function

$$J(\mathbf{p}, \mathbf{k}) = \frac{\beta(\mathbf{p} - \mathbf{k})}{|\mathbf{p} - \mathbf{k}|}, \tag{7}$$

where

$$\beta(\mathbf{q}) = \frac{1}{1 + \frac{N_f}{2}\alpha\left[\frac{2m_1}{|\mathbf{q}|} + \frac{\mathbf{q}^2 - 4m_1^2}{\mathbf{q}^2}\arctan\left(\frac{|\mathbf{q}|}{2m_1}\right)\right]}. \tag{8}$$

N_f is the number of spin flavor and will be taken to be 2 in this paper. We approximate the kernel by its asymptotic value at $p \ll k$ and $p \gg k$, so that

$$J(p, k) = \theta(p - k)\frac{\beta(\mathbf{p})}{p} + \theta(k - p)\frac{\beta(\mathbf{k})}{k}. \tag{9}$$

Therefore the gap equation (6) is written in the form

$$\Delta_1(p) = m_1 + \frac{\alpha}{\pi} \int_0^\Lambda dk\, J(p, k) \frac{k\Delta_1(k)}{\sqrt{k^2 + \Delta_1(k)^2}}, \tag{10}$$

where Λ is upper momentum cutoff with the order of the inverse of the lattice constant. Here we choose its value as 10 eV.

In the present work, we solve the integral equation numerically. From $\Delta(p)$, the chiral condensate $\langle \text{vac}|\bar{\psi}_s \psi_{s'}|\text{vac}\rangle$ can be evaluated by its definition[11]

$$\langle \text{vac}|\bar{\psi}_s \psi_{s'}|\text{vac}\rangle = -\text{tr} \lim_{x \to 0} \langle \text{vac}|T\psi_{s'}(x)\bar{\psi}_s(0)|\text{vac}\rangle$$

$$= -\text{tr} \int \frac{dp_0}{2\pi} \frac{d^2p}{(2\pi)^2} \frac{i}{\not{p} - \Delta_s} \delta_{ss'}$$

$$= -\frac{1}{\pi} \int_0^\Lambda \frac{\Delta_s(p) p\, dp}{\sqrt{p^2 + \Delta_s(p)^2}} \delta_{ss'}. \tag{11}$$

The numerical results for chiral condensate $\langle \text{vac}|\bar{\psi}_s \psi_{s'}|\text{vac}\rangle = \delta_{ss'}\langle \bar{\psi}\psi \rangle$ and dynamical fermion mass at zero momentum $\Delta(0)$ are presented in Table I for the case of zero bare mass $m = 0$ and in Table II for the case of small bare mass $m = 1.00 \times 10^{-7} \Lambda$. Comparing these two tables, it is easy to see that the small bare mass of the Dirac fermion leads to a substantial enhancement of the chiral condensate. When interaction strength $\alpha = 5$, the dynamical mass $\Delta(0)$ in Table II is nearly 20 times larger than the value of dynamical mass in

TABLE I. Numerical results of chiral condensate without bare mass. Here, the chiral condensate is $\rho = -\langle \bar{\psi}\psi \rangle / \Lambda^2$.

α	2.4	2.5	5	10	∞
ρ	0	1.34(−31)	1.84(−9)	2.22(−7)	4.57(−6)
$\Delta(0)/\Lambda$	0	2.67(−21)	1.70(−6)	4.37(−5)	3.45(−4)

Table I, while the chiral condensate is about 100 times larger. When there is no bare fermion mass, there is no excitonic pairing and the Dirac fermions remain massless for $\alpha \leqslant 2.4$. The critical strength α_c of the Coulomb interaction lies in the interval of $(2.4, 2.5)$, which is a little larger than the result of Ref. [11]. However, when the Dirac fermions have a small bare mass, excitonic pairing and DCSB can take place for any non-zero value of α. For graphene placed on SiO_2 with $\alpha \approx 0.8$,[12,18] the dynamical fermion mass $\Delta(0) = 2.15 \times 10^{-6}\Lambda$ comes mainly from the formation of excitonic pairs since it is much larger than the bare mass $1.00 \times 10^{-7}\Lambda$.

In summary, the small bare fermion mass has two effects: It reduces the critical Coulomb interaction strength α_c and enhances the magnitude of dynamical fermion mass $\Delta(0)$. These effects are important from both experimental and technical points of view. On the one hand, the fermion gap can be detected unambiguously in experiments only when it is sufficiently large.[18] On the other hand, the graphene material with a large gap will have more technical advantages than that without fermion gap.[18]

We would like to emphasize that, although the bare fermion mass can catalyze the generation of dynamical fermion mass, the latter is physically different from the bare mass. In this work, the bare mass is assumed to be generated by several possible mechanisms and small in quantity. It can be non-zero even when the Coulomb interaction between Dirac fermions is completely ignored. However, the dynamical fermion mass originates from the formation of chiral vacuum condensate driven by Coulomb interaction and thus is a typical effect of strong correlation between fermions.

It is also interesting to compare the excitonic pair formation with the Cooper pair formation in the BCS theory of superconductivity. Historically, the proposal of dynamical chiral symmetry breaking of Nambu and Jona-Lasinio was motivated by the BCS theory. However, there are essential differences between them. An excitonic pair is composed of a particle and a hole, and thus is neutral. On the contrary, a Cooper pair is composed of two electrons, and thus carries negative charge $-2e$. Moreover, the formation of excitonic pairs breaks chiral symmetry and leads to insulating behavior, whereas the formation of Cooper pairs breaks local gauge symmetry and leads to superconductivity.

The DS equation with a Kekule-distortion-induced fermion mass was studied previously in Ref. [16], which concludes that the dynamical mass generation due to interaction is independent of the homogeneous Kekule distortion. In Ref. [16], an important claim was that the gap equation is dominated by the large momentum regime. However, it is known that dynamical chiral symmetry breaking is a nonperturbative, low-energy phenomenon. This phenomenon can happen only when the interaction between fermions is weak at the high energy/momentum regime and strong at the low

energy/momentum regime (i.e., asymptotic freedom). Therefore the processes with small energy/momentum transfer should play dominant role in the formation of excitonic pairing. According to our numerical computation, the dynamical mass generation is indeed significantly affected by the presence of homogeneous Kekule distortion whose catalytic effect can be readily seen from the comparison of Tables I and II.

In the calculation presented below, we will need the normal-ordered chiral condensate $\langle \text{vac}| : \bar{\psi}(0)\psi(0) : |\text{vac}\rangle = \langle \text{vac}|\bar{\psi}(0)\psi(0)|\text{vac}\rangle - \langle \Omega|\bar{\psi}(0)\psi(0)|\Omega\rangle$. Quite different from the nonperturbative symmetry-broken vacuum state $|\text{vac}\rangle$, $|\Omega\rangle$ is the perturbative vacuum state that is chiral symmetric.[40] As a function of α, the value of $\langle \text{vac}| : \bar{\psi}(0)\psi(0) : |\text{vac}\rangle$ will be specified in Sec. III.

III. SVZ SUM-RULE ANALYSIS OF GOLDSTONE-TYPE EXCITONS

Since the Dirac fermions have a small bare mass, the Lagrangian of graphene respects an approximate continuous chiral symmetry. As emphasized by Weinberg,[19] when an approximate continuous symmetry is broken, the Goldstone bosons are no longer massless. Instead, these bosons are massive. In the context of graphene, the Goldstone-type excitons induced by dynamical breaking of approximate chiral symmetry have finite masses. In this section, we calculate the masses of these excitons and compare them with the dynamical fermion mass.

An exciton is a boson composed of a Dirac particle and a Dirac hole (i.e., an antifermion in the terminology of particle physics). It can be described by a composite operator of spinor field and its conjugate. For graphene, when chiral condensate occurs $\langle \bar{\psi}\psi \rangle \neq 0$, the chiral symmetry U(4) is broken down to $U(2) \times U(2)$ and the number of broken generators is 8. The eight corresponding Goldstone bosons can be described by $\bar{\psi}\gamma_3 \otimes \sigma_\mu \psi$ and $\bar{\psi}i\gamma_5 \otimes \sigma_\mu \psi$,[32,41] where σ_0 is the unit matrix. The modes of $\bar{\psi}i\gamma_5 \otimes \sigma_\mu \psi$ are bond-density waves that mix the K and K' points, similar to the Kekule distortion mode $\langle \bar{\psi}\psi \rangle$.[15,39] $\bar{\psi}\gamma_3 \otimes \sigma_\mu \psi$ is related to the CDW or staggered SDW excitations.[3]

In this section, we will calculate the masses of the lowest-energy excitons corresponding to $\phi_0 = \bar{\psi}\gamma_3 \otimes \sigma_0 \psi$ and $\phi_i = \bar{\psi}\gamma_3 \otimes \sigma_i \psi$ using the SVZ sum-rule method, which is analogous to the procedure of computing pion mass in particle physics.[25] This procedure can also be applied to the excitons associated with $\bar{\psi}i\gamma_5 \otimes \sigma_\mu \psi$ and the results are the same, so we will not discuss the case of $\bar{\psi}i\gamma_5 \otimes \sigma_\mu \psi$. The basic idea of the SVZ sum rule is to compute one particular physical quantity in two different ways and then extract important information of some parameter (such as the mass of a Goldstone boson) by equating the expressions obtained by different ways. In the present problem, the physical quantities

TABLE II. Numerical results of chiral condensate with bare mass $m = 10^{-7}\Lambda$.

α	0	0.8	1	2	2.2	2.4	2.5	5	10	∞
ρ	3.20(−8)	5.40(−8)	5.91(−8)	8.57(−8)	9.17(−8)	9.78(−8)	1.01(−7)	2.13(−7)	6.37(−7)	5.12(−6)
$\Delta(0)/\Lambda$	1.00(−7)	2.15(−6)	3.00(−6)	8.37(−6)	9.62(−6)	1.09(−5)	1.16(−5)	3.12(−5)	8.19(−5)	3.67(−4)

to be computed are the correlation functions of composite fields ϕ_0 and ϕ_i. To apply the SVZ sum-rule technique, the OPE method will be used to separate the perturbative and nonperturbative contributions to the correlation function. The perturbative contributions are included in the so-called Wilson's coefficients and can be calculated perturbatively. The nonperturbative contributions are embodied as chiral condensates, which can be obtained from experimental data or calculated by some nonperturbative methods. In our case, the condensates are calculated by means of the DS equation method.

We first consider the field ϕ_0. Its correlation function is defined as

$$\Pi(q) = i \int d^3x e^{iqx} \langle \text{vac}|T\phi_0(x)\phi_0^\dagger(0)|\text{vac}\rangle, \quad (12)$$

where $|\text{vac}\rangle$ is the nonperturbative vacuum state in the chiral symmetry-breaking phase. Substituting the four components of ψ, we have

$$\phi_0 \sim \sum_s A_s^+(K)A_s(K) + A_s^+(K')A_s(K')$$
$$- B_s^+(K)B_s(K) - B_s^+(K')B_s(K') = N_A - N_B, \quad (13)$$

which corresponds to the CDW excitation. In order to get information of the excitation, the correlation function will be calculated in two different ways: phenomenologically and theoretically. On the phenomenological side, the correlation function is related to physical observables, while on the theoretical side the same function is expressed in terms of fundamental parameters such as m and α which are treated as known numbers. Equating the results obtained in these two ways, we can obtain the expression for exciton masses in terms of fundamental parameters.

To perform the phenomenological computation, we insert a complete set of physical states, $1 = \sum_n |n,p_n\rangle d\tau_n \langle n,p_n|$, between the two operators in Eq. (12). Here, p_n is the momentum of the intermediate state and $d\tau_n = d^3p_n\delta(p_n^2 - M_n^2)\theta(p_n^0)/(2\pi)^2$ denotes the integration over phase space.[42] The index n can take both discrete and continuous values, which implies that both discrete bound states and continuous states are included. After integrating out space and momentum coordinates, we obtain

$$\text{Im}\Pi(q) = \sum_n \pi\delta(q^2 - M_n^2)F_n, \quad (14)$$

where $F_n = |\langle n,q|\phi_0|\text{vac}\rangle|^2$. M_n is the mass of the intermediate state $|n\rangle$ or the static energy in its rest reference system. For later convenience, we now introduce a function $\widetilde{\Pi}(q^2)$, defined by

$$\Pi(q) = q^2\widetilde{\Pi}(q^2), \quad (15)$$

and then have

$$\text{Im}\widetilde{\Pi}(q^2) = \pi f_{\varphi_0}\delta(q^2 - m_{\varphi_0}^2) + \sum_n \pi f_n\delta(q^2 - M_n^2) \quad (16)$$

with $F_n = M_n^2 f_n$. Here we have isolated the contribution of the lowest-lying state φ_0. The mass of φ_0, m_{φ_0}, gives the position of the corresponding resonance. In the context of particle physics, f_{φ_0} is called the decay constant of the bound

state. In the context of graphene, it is related to the strength of exciton resonance. The second term of the right-hand side of Eq. (16) includes both discrete and continuous states. Using the dispersion relation

$$\widetilde{\Pi}(q^2) = \frac{1}{\pi}\int_0^{+\infty} ds \frac{\text{Im}\widetilde{\Pi}(s)}{s - q^2 - i\epsilon}, \quad (17)$$

we obtain

$$\widetilde{\Pi}(q^2) = \frac{f_{\varphi_0}}{m_{\varphi_0}^2 - q^2} + \sum_n \frac{f_n}{M_n^2 - q^2}, \quad (18)$$

where the first term is the contribution of the lowest-lying state and the second term is the contribution of higher excited states.

In order to identify the mass m_{φ_0} of the lowest-lying exciton state corresponding to $\bar\psi\gamma_3\psi$, we need to perform the theoretical analysis starting from the same correlation function. The correlation function can be calculated by means of the OPE method, which is able to account for the nonperturbative effects due to chiral-symmetry broken vacuum. We first write down the following expression:

$$i \int d^3x e^{iqx} T\phi_0(x)\phi_0^\dagger(0)$$
$$= C_0(q) + C_{2,1}(q) : \bar\psi_1\psi_1(0) : + C_{2,2}(q) : \bar\psi_2\psi_2(0) :$$
$$+ C_4(q) : \bar\psi\Gamma\psi\bar\psi\Gamma'\psi(0) : + \cdots. \quad (19)$$

The Wilson's coefficients C_n's contain the perturbative contributions, while the operators multiplying C_n's contain the nonperturbative contributions. From dimension analysis, we know that the mass dimension of the left-hand side of Eq. (19) is 1, so each term in the right-hand side should have the same dimension. Since the operators appearing in the right-hand side are all local operators with increasing mass dimensions, the mass dimension of C_n should decrease with n. This indicates that C_n's contain increasing powers of $1/q^2$ as n grows. After taking the vacuum expectation value, the contributions of higher terms are suppressed by $\langle : \bar\psi\psi : \rangle/q^2$ for large q^2. In the present work, we are mainly interested in the region $-q^2 \gg |\langle : \bar\psi\psi : \rangle|$ in Eq. (19) and thus can keep only the first three terms. Generally speaking, C_n can be obtained by sandwiching the two sides of Eq. (19) with a pair of states and comparing the results from both sides, as shown by Braaten.[27] Here for C_0, we sandwich Eq. (19) by the perturbative vacuum state $|\Omega\rangle$, which eliminates the contributions of higher terms. Therefore C_0 will be calculated by evaluating the Feynman diagram of a fermion loop. For $C_{2,1}$ and $C_{2,2}$, following the works of Refs. 42 and 43, we sandwich Eq. (19) by nonperturbative vacuum state $|\text{vac}\rangle$ and apply Wick's theorem to the left-hand side. Then a pair of fermionic operators are contracted. After calculating the tree-level Feynman diagram and matching the two sides, we will get $C_{2,1}$ and $C_{2,2}$. Furthermore, perturbative calculations for Wilson's coefficients are performed in the framework of $1/N_f$ expansion and only leading term $C_n^{(0)}$'s are kept in the present work.

Sandwiching Eq. (19) by the physical vacuum state, one obtains

$$\Pi(q) = C_0^{(0)}(q) + C_{2,1}^{(0)}(q)\langle : \bar\psi_1\psi_1 : \rangle + C_{2,2}^{(0)}(q)\langle : \bar\psi_2\psi_2 : \rangle. \quad (20)$$

Similar to the relation between Π and $\widetilde{\Pi}$, we introduce $\widetilde{C}_n^{(0)}$'s satisfying

$$C_n^{(0)}(q) = q^2 \widetilde{C}_n^{(0)}(q^2), \tag{21}$$

and then we have

$$\widetilde{\Pi}(q^2) = \widetilde{C}_0^{(0)}(q^2) + \widetilde{C}_{2,1}^{(0)}(q^2)\langle : \bar{\psi}_1 \psi_1 : \rangle + \widetilde{C}_{2,2}^{(0)}(q^2)\langle : \bar{\psi}_2 \psi_2 : \rangle. \tag{22}$$

Since $\mathrm{Im} C_0^{(0)}$ can be obtained from evaluating the imaginary part of a fermionic loop diagram, we obtain

$$\mathrm{Im}\widetilde{C}_0^{(0)}(q^2) = \frac{1}{4\sqrt{q^2}}\theta(q^2 - 4m_1^2) + \frac{1}{4\sqrt{q^2}}\theta(q^2 - 4m_2^2). \tag{23}$$

$C_{2,i}^{(0)}$ ($i = 1,2$) can be obtained by directly computing the tree diagrams, with the expression

$$C_{2,i}^{(0)}(q^2) = \frac{4m_i q^2}{3(q^2 - m_i^2)^2} \simeq \frac{4m_i}{3q^2}, \tag{24}$$

in the region $Q^2 = -q^2 \gg m^2$.

Equating the right-hand sides of Eqs. (18) and (22) and substituting C_n's, we obtain

$$\frac{f_{\varphi_0}}{Q^2 + m_{\varphi_0}^2} + \sum_n \frac{f_n}{Q^2 + M_n^2}$$
$$= \frac{1}{\pi}\int ds \frac{\mathrm{Im}\widetilde{C}_0^{(0)}(s)}{s + Q^2 - i\epsilon} + \frac{4m_1 \langle : \bar{\psi}_1 \psi_1 : \rangle}{3(Q^2)^2}$$
$$+ \frac{4m_2 \langle : \bar{\psi}_2 \psi_2 : \rangle}{3(Q^2)^2} + \mathcal{O}\left(\frac{1}{Q^6}\right). \tag{25}$$

In order to extract the information of the lowest-lying state, it is helpful to introduce the Borel transformation

$$\mathcal{B}_{M^2} = -\lim_{Q^2 = nM^2 \to \infty} \frac{(-Q^2)^{n+1}}{n!}\left(\frac{d}{dQ^2}\right)^n, \tag{26}$$

which can suppress the contribution from more massive states on the left-hand side of Eq. (25). Now we can obtain the sum rule

$$f_{\varphi_0} e^{-m_{\varphi_0}^2/M^2} + \sum_n f_n e^{-M_n^2/M^2} = \frac{1}{\pi}\int ds \mathrm{Im}\widetilde{C}_0^{(0)}(s)e^{-s/M^2}$$
$$- \frac{2X}{3M^2} + \mathcal{O}\left(\frac{1}{M^4}\right), \tag{27}$$

where

$$X = -2m_1 \langle : \bar{\psi}_1 \psi_1 : \rangle - 2m_2 \langle : \bar{\psi}_2 \psi_2 : \rangle. \tag{28}$$

The contribution from higher states is suppressed exponentially and seems to be unimportant. However, these higher states include continuous ones, so they cannot be simply neglected. We assume that the continuous states begin at $2\Delta(p = 0)$, with $\Delta(0)$ being the dynamical fermion mass, and subtract their contribution from both sides of Eq. (27), which is an analog to the quark-hadron duality in particle

physics.[22,42,44,45] The resultant expression is

$$\frac{1}{\pi}\int_0^{(2\Delta)^2} ds \mathrm{Im}\widetilde{\Pi}(s)e^{-s/M^2} = \frac{1}{\pi}\int_0^{(2\Delta)^2} ds \mathrm{Im}\widetilde{C}_0^{(0)}(s)e^{-s/M^2}$$
$$- \frac{2X}{3M^2} + \mathcal{O}\left(\frac{1}{M^4}\right), \tag{29}$$

In this expression, X contains the normal-ordered condensates, which were not specified in Sec. II. Here we define them as

$$\langle \mathrm{vac}| : \bar{\psi}_1 \psi_1 : |\mathrm{vac}\rangle = -\frac{1}{\pi}\int_0^{2\Delta_1(0)} \frac{\Delta_1(p)p dp}{\sqrt{p^2 + \Delta_1(p)^2}}, \tag{30}$$

and $\langle : \bar{\psi}_2 \psi_2 : \rangle$ can be defined similarly. From the numerical results of $\Delta(p)$ obtained Sec. II, the value of $\langle : \bar{\psi}\psi : \rangle$ can be computed by numerical integration. Then we obtain the sum-rule formula

$$f_{\varphi_0} e^{-m_{\varphi_0}^2/M^2} + \cdots = \frac{1}{2\pi}\int_{2m_1}^{2\Delta_1} e^{-u^2/M^2} du + \frac{4m_1 \langle : \bar{\psi}_1 \psi_1 : \rangle}{3M^2}$$
$$+ (1 \leftrightarrow 2) + \mathcal{O}\left(\frac{1}{M^4}\right), \tag{31}$$

where $\cdots$ is the contribution from the discrete higher states and is neglected altogether. Differentiating the above expression with respect to $\eta = 1/M^2$ and introducing the ratio between the derivative and Eq. (31), we eventually obtain the sum rule for the mass of exciton φ_0:

$$m_{\varphi_0}^2 = \frac{\int_{2m_1}^{2\Delta_1} u^2 e^{-u^2\eta} du - \frac{8\pi}{3}m_1 \langle : \bar{\psi}_1 \psi_1 : \rangle + (1 \leftrightarrow 2)}{\int_{2m_1}^{2\Delta_1} e^{-u^2\eta} du + \frac{8\pi}{3}m_1 \langle : \bar{\psi}_1 \psi_1 : \rangle\eta + (1 \leftrightarrow 2)}. \tag{32}$$

Besides, the sum-rule formula for f_{φ_0} is

$$f_{\varphi_0} = e^{m_{\varphi_0}^2\eta}\left[\frac{1}{2\pi}\int_{2m_1}^{2\Delta_1} e^{-u^2\eta} du + \frac{4m_1 \langle : \bar{\psi}_1 \psi_1 : \rangle}{3}\eta + (1 \leftrightarrow 2)\right]. \tag{33}$$

We next consider the correlation function of $\phi_1 = \bar{\psi}_1 \gamma_3 \psi_2 \sim A_\uparrow^\dagger A_\downarrow - B_\uparrow^\dagger B_\downarrow$. Analogously, we define

$$\Pi_1(q) = i\int d^3 x e^{iqx}\langle \mathrm{vac}|T\phi_1(x)\phi_1^\dagger(0)|\mathrm{vac}\rangle, \tag{34}$$

which is the counterpart of the transverse component of the staggered spin susceptibility investigated in the context of high-temperature cuprate superconductors.[46] A similar OPE is applied to $\Pi_1(q)$, and the results for the corresponding coefficients are

$$\mathrm{Im}\widetilde{C}_0^{(0)}(q^2) = \frac{1}{4\sqrt{q^2}}\theta(q^2 - 4m^2) \tag{35}$$

with $m = (m_1 + m_2)/2$. The resulting sum-rule formula after Borel transformation is

$$f_{\varphi_1} e^{-m_{\varphi_1}^2/M^2} + \cdots = \frac{1}{2\pi}\int_{2m}^{2\Delta} e^{-u^2/M^2} du$$
$$+ \left[\frac{(3m_2 - m_1)\langle : \bar{\psi}_1 \psi_1 : \rangle}{3M^2} + (1 \leftrightarrow 2)\right]$$
$$+ \mathcal{O}\left(\frac{1}{M^4}\right). \tag{36}$$

Differentiate it with respect to $\eta = 1/M^2$ then one gets the sum-rule formula for the mass of exciton φ_1:

$$m_{\varphi_1}^2 = \frac{\int_{2m}^{2\Delta} u^2 e^{-u^2\eta} du - \left[\frac{2\pi}{3}(3m_2 - m_1)\langle : \bar\psi_1\psi_1 : \rangle + (1 \leftrightarrow 2)\right]}{\int_{2m}^{2\Delta} e^{-u^2\eta} du + \left[\frac{2\pi}{3}(3m_2 - m_1)\langle : \bar\psi_1\psi_1 : \rangle\eta + (1 \leftrightarrow 2)\right]}$$ (37)

with $2m = m_1 + m_2$ and $2\Delta = \Delta_1(0) + \Delta_2(0)$.

The sum-rule formulas for the masses of excitons ϕ_2 and ϕ_3 can be derived similarly. The formula for m_{φ_2} is exactly the same as m_{φ_1}, Eq. (37). For ϕ_3, one considers the following two-point correlation function:

$$\Pi_3(q) = i \int d^3x e^{iqx} \langle \text{vac}|T\phi_3(x)\phi_3(0)|\text{vac}\rangle,$$ (38)

where ϕ_3 is the longitudinal component of the staggered SDW, given by

$$\phi_3 \sim (N_{A\uparrow} - N_{A\downarrow}) - (N_{B\uparrow} - N_{B\downarrow}).$$ (39)

The sum-rule formula for m_{φ_3} is the same as m_{φ_0}, which is presented above.

In our truncated computation, these sum-rule formulas for the exciton masses Eqs. (32) and (37) are functions of the Borel parameter M or η. In order to fix the value m_φ for exciton φ, we need a criterion for the choice of η and the corresponding $m_\varphi(\eta)$. In the sum-rule literature, the optimum estimate value may be determined by an extreme value, an inflection point[43,47] or a plateau[42] of the function. In the present work, we choose a plateau near the extreme value of the function to be the final output for m_φ or f_φ.

For $m_1 = m_2 = 1.00 \times 10^{-7}\Lambda$ and $\alpha = 0.8$ (SiO$_2$ case), the numerical results for the chiral condensate and mass gap are $-\langle : \bar\psi_1\psi_1 : \rangle = -\langle : \bar\psi_2\psi_2 : \rangle = 1.70 \times 10^{-12}\Lambda^2$ and $\Delta(0) = 2.15 \times 10^{-6}\Lambda$. The cutoff scale Λ is normally set as 10 eV. From these quantities, the SVZ estimates for the masses of the excitons can be made with the criterion discussed above: φ_0, φ_1, φ_2, and φ_3 have the same mass, 0.028 meV. For $m_1 \neq m_2$, the fourfold mass degenerate is lifted to twofold: φ_1 and φ_2 have the same mass, which is a little smaller than m_{φ_0} and m_{φ_3}. For the case of suspended graphene, $\alpha = 2.2$, we have $-\langle : \bar\psi\psi : \rangle = 3.33 \times 10^{-11}\Lambda^2$, $\Delta(0) = 9.62 \times 10^{-6}\Lambda$. Now the mass of φ particles is about 0.098 meV.

It is now necessary to summarize and compare the relevant energy scales discussed above. The fundamental energy scale in the present problem is the ultraviolet cutoff $\Lambda = 10$ eV in graphene, which is normally determined by the lattice constant. In this paper, we assume a bare fermion mass $m = 1.00 \times 10^{-7}\Lambda$, which may be generated by Kekule distortion or other mechanisms. All other energy scales are derived by explicit calculations. We note here that the exciton mass is smaller than $2\Delta(0)$, which implies that the binding energy of the bound state is negative.

IV. SPIN SUSCEPTIBILITY AND NON-GOLDSTONE-TYPE EXCITONS

In addition to the CDW and staggered SDW excitons studied in the last section, there is another kind of low-energy collective excitations: spin excitons. These spin excitons are not generated due to chiral symmetry breaking and thus are non-Goldstone-type bosons. In the absence of any (bare or dynamical) fermion mass, these spin excitons are massless in clean graphene[48,49] and become massive in doped graphene.[50] In the present problem, the fermions have finite dynamical mass in the chiral-symmetry-broken phase, so the spin excitons are also massive. In order to study these triplet spin-1 excitons, we turn to study the spin susceptibilities, which may be measured by inelastic neutron scattering.[49] These quantities were studied previously in an effective QED$_3$ theory of high-temperature superconductors.[51]

In this section, we will calculate the masses of spin excitons using the methods presented in the last section. To do this, we first define the spin operator as $S_i = \psi_a^\dagger \sigma_{ab}^i \psi_b$, where σ^i ($i = x, y, z$) are Pauli matrices and a and b are spin indices. The transverse and longitudinal spin susceptibilities are defined as

$$\chi_{+-}(q) = i \int d^3x e^{iqx} \langle \text{vac}|T S_+(x)S_-(0)|\text{vac}\rangle,$$ (40)

and

$$\chi_{zz}(q) = i \int d^3x e^{iqx} \langle \text{vac}|T S_z(x)S_z(0)|\text{vac}\rangle,$$ (41)

respectively. Here, $|\text{vac}\rangle$ is the nonperturbative physical vacuum state of the system in the chiral-symmetry-broken phase. The quantity χ_{-+} can be similarly studied and will not be discussed here.

The spin susceptibility will be computed by means of the SVZ sum-rule method. We note that Rosenfelder applied the SVZ sum-rule method to analyze the density-density correlation function and estimate the position of plasmon resonance in a nonrelativistic electron system.[26] In our case, the spin susceptibility will be analyzed in both phenomenological and theoretical ways, analogous to what we have done in the last section.

On the phenomenological side, following the previous work,[48–51] we assume that there is a resonance below the spin gap. This assumption is embodied in the expression

$$\frac{1}{\pi}\text{Im}\chi_l(p) = F_\sigma \delta(p^2 - m_\sigma^2) + \sum_n F_n \delta(p^2 - \mu_n^2)$$
$$+ \Theta(p^2 - U_{\text{sg}})\rho_\sigma(p^2),$$ (42)

where the first δ-function-type resonance σ corresponds to the so-called spin exciton. $\sigma = +, -, z$ for $l = +-, -+, zz$, respectively. The spin gap U_{sg} is the lower bound of the continuous spectrum. The second term is the contribution from the discrete excited bound states, whose masses μ_n's are either between m_σ and U_{sg} or larger than U_{sg}. From the dispersion relation formula, we obtain that, for $p^2 < 0$,

$$\chi_l(p^2) = \frac{1}{\pi} \int_0^\infty ds \frac{\text{Im}\chi_l(s)}{s - p^2 - i\epsilon}$$
$$= \frac{F_\sigma}{m_\sigma^2 - p^2} + \sum_n \frac{F_n}{\mu_n^2 - p^2} + \int_{U_{\text{sg}}}^{+\infty} \frac{\rho_\sigma(s)ds}{s - p^2}.$$ (43)

To compute the same correlation function theoretically, the OPE is adopted to take into account the nonperturbative

effects due to chiral symmetry breaking. For transverse spin susceptibility, we have

$$
\begin{aligned}
i \int & d^3 x e^{ipx} T S_+(x) S_-(0) \\
&= D_0(p) + D_{2,1}(p) : \bar{\psi}_1 \psi_1(0) : + D_{2,2}(p) : \bar{\psi}_2 \psi_2(0) : \\
&\quad + D_4(p) : \bar{\psi} \Gamma \psi \bar{\psi} \Gamma' \psi(0) : + \cdots .
\end{aligned} \tag{44}
$$

As explained in Sec. III, the operators in the right-hand side are all local operators, so the contributions of this series are suppressed by powers of $\langle : \bar{\psi}\psi : \rangle / q^2$. Therefore we can keep only the first three terms. Sandwiching Eq. (44) by the physical vacuum state, we have

$$
\begin{aligned}
\chi_{+-}(p) = {}& D_0^{(0)}(p) + D_{2,1}^{(0)}(p)\langle : \bar{\psi}_1 \psi_1 : \rangle \\
&+ D_{2,2}^{(0)}(p)\langle : \bar{\psi}_2 \psi_2 : \rangle + \cdots .
\end{aligned} \tag{45}
$$

D_n can be obtained by perturbative expansion computation and each D_n is a power series in coupling α, therefore only the leading terms of $D_n^{(0)}$ are important. For $D_0^{(0)}$, its imaginary part is

$$
\begin{aligned}
\mathrm{Im} D_0^{(0)}(p^2, \mathbf{p}^2) = {}& \Theta(p^2 - 4m^2)\frac{\mathbf{p}^2}{8\sqrt{p^2}} \\
&+ \Theta(p^2 - 4m^2)\frac{m^2 \mathbf{p}^2}{2p^2\sqrt{p^2}}.
\end{aligned} \tag{46}
$$

After calculating the coefficients D_n's in Eq. (45), we get the truncated expression of transverse spin susceptibility for the case $m_1 = m_2$, as follows:

$$
\chi_{+-}(p^2, \mathbf{p}) = \frac{1}{\pi} \int_0^\infty ds \frac{\mathrm{Im} D_0^{(0)}(s)}{s - p^2 - i\epsilon} + \frac{8m\langle : \bar{\psi}\psi : \rangle \mathbf{p}^2}{3(-p^2)^2}, \tag{47}
$$

where $\langle : \bar{\psi}\psi : \rangle = \langle : \bar{\psi}_1 \psi_1 : \rangle = \langle : \bar{\psi}_2 \psi_2 : \rangle$ and $-p^2 \gg m^2$. Note that all terms with higher order of m^2/p^2 are ignored.

Equating the right-hand sides of Eqs. (43) and (47), we get a sum-rule formula,

$$
\begin{aligned}
\frac{1}{\pi} \int_0^\infty ds \frac{\mathrm{Im}\chi_{+-}(s)}{s - p^2 - i\epsilon} = {}& \frac{1}{\pi} \int_0^\infty ds \frac{\mathrm{Im} D_0^{(0)}(s)}{s - p^2 - i\epsilon} \\
&+ \frac{8m\langle : \bar{\psi}\psi : \rangle \mathbf{p}^2}{3(-p^2)^2}.
\end{aligned} \tag{48}
$$

In order to subtract the contribution from the states beyond the spin gap in both sides of the above equation, duality is used and the upper cutoff is replaced by $(2\Delta)^2$, so that

$$
\begin{aligned}
\frac{1}{\pi} \int_0^{(2\Delta)^2} ds \frac{\mathrm{Im}\chi_{+-}(s)}{s - p^2 - i\epsilon} = {}& \frac{1}{\pi} \int_0^{(2\Delta)^2} ds \frac{\mathrm{Im} D_0^{(0)}(s)}{s - p^2 - i\epsilon} \\
&+ \frac{8m\langle : \bar{\psi}\psi : \rangle \mathbf{p}^2}{3(-p^2)^2}.
\end{aligned} \tag{49}
$$

In this expression, the value of $\langle : \bar{\psi}\psi : \rangle$ was given by Eq. (30). Now we can obtain the following sum-rule formula:

$$
\begin{aligned}
\frac{F_+}{m_+^2 - p^2} + \cdots = {}& \frac{1}{\pi} \int_0^{(2\Delta)^2} ds \frac{\mathrm{Im} D_0^{(0)}(s)}{s - p^2 - i\epsilon} \\
&- \frac{8m\mathbf{p}^2}{3(-p^2)^2} \frac{1}{\pi} \int_0^{(2\Delta)^2} \frac{\Delta(s)ds}{\sqrt{s + \Delta(s)^2}},
\end{aligned} \tag{50}
$$

where $\cdots$ stands for the contribution from the discrete excited bound states. Furthermore, in order to extract the information of the lowest-lying state, Borel transformation can be used to suppress the contribution from excited states in the left-hand side of Eq. (50), leading to

$$
\begin{aligned}
F_+ e^{-m_+^2/M^2} &+ \sum_n F_n e^{-\mu_n^2/M^2} \\
&= \frac{\mathbf{p}^2}{4\pi} \int_{2m}^{2\Delta} e^{-\tau^2/M^2} d\tau + \frac{8m\langle : \bar{\psi}\psi : \rangle}{3M^2}\mathbf{p}^2 + \mathcal{O}\left(\frac{1}{M^4}\right).
\end{aligned} \tag{51}
$$

The second term of the left-hand side of the above equation is the contribution from the more massive states, which is suppressed exponentially and will be neglected altogether in the following. Differentiating the above expression with respect to $\eta = M^2$, we get the following sum-rule formula for mass m_+ of the spin exciton:

$$
m_+^2 = \frac{\int_{2m}^{2\Delta} \tau^2 e^{-\tau^2\eta} d\tau - \frac{32\pi}{3}m\langle : \bar{\psi}\psi : \rangle}{\int_{2m}^{2\Delta} e^{-\tau^2\eta} d\tau + \frac{32\pi}{3}m\langle : \bar{\psi}\psi : \rangle\eta}. \tag{52}
$$

The sum-rule formula for m_- is exactly the same as m_+. In addition, the longitudinal spin susceptibility χ_{zz} can be analyzed similarly. When $-p^2 \gg m^2$, the OPE result of $\chi_{zz}(p^2, \mathbf{p})$ is

$$
\begin{aligned}
\chi_{zz}(p^2, \mathbf{p}) = {}& \frac{2}{\pi} \int_0^\infty ds \frac{\mathrm{Im} D_0^{(0)}(s)}{s - p^2 - i\epsilon} \\
&+ \frac{8m_1\langle : \bar{\psi}_1 \psi_1 : \rangle + 8m_2\langle : \bar{\psi}_2 \psi_2 : \rangle}{3(-p^2)^2}\mathbf{p}^2.
\end{aligned} \tag{53}
$$

The final sum-rule formula for the associated quantity m_z^2 will have the same form as Eq. (52) in the case of $m_1 = m_2$. Apparently, the three spin excitons are mass degenerated.

In our truncated computation, the sum-rule formula for the exciton masses Eq. (52) is a function of the Borel parameter
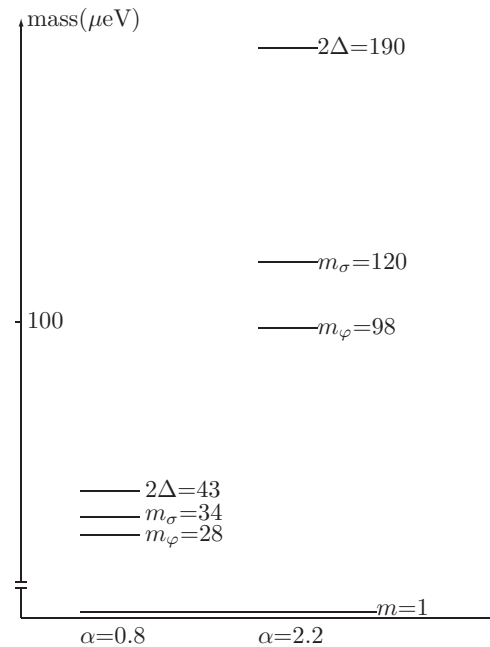

FIG. 1. Typical mass scales for effective fermion gap 2Δ, CDW exciton m_φ and spin exciton m_σ. The bare fermion mass m is chosen as 1 μeV.

M or η. These two parameters are determined in the same way presented in Sec. III. For $m_1 = m_2 = 10^{-7}\Lambda$ and $\alpha = 0.8$ (SiO$_2$ case), the numerical results for the chiral condensate are $-\langle: \bar{\psi}_1\psi_1 :\rangle = -\langle: \bar{\psi}_2\psi_2 :\rangle = 1.70 \times 10^{-12}\Lambda^2$. From these quantities, the SVZ estimation for the mass of the spin excitons is $m_\sigma = 0.034$ meV. For suspended graphene with $\alpha = 2.2$, $-\langle: \bar{\psi}\psi :\rangle = 3.33 \times 10^{-11}\Lambda^2$ and the estimated value for the spin exciton mass is 0.12 meV.

The typical masses obtained above are illustrated in Fig. 1. Comparing these masses, we see that the spin excitons are more massive than Goldstone-type excitons, while their masses are smaller than $2\Delta(0)$, which is consistent with the assumption made before Eq. (42). It is interesting to compare our results shown in Fig. 1 with the Fig. 3 of the first paper of Ref. 10, where the masses of pionlike excitons were calculated in the framework of lattice gauge theory.

V. SUMMARY AND CONCLUSION

In this paper, we studied the dynamical breaking of approximate chiral symmetry in graphene and calculated the spectra of both Goldstone-type and non-Goldstone-type excitons. In the presence of a small bare fermion mass, the critical Coulomb interaction strength α_c for dynamical fermion mass generation is reduced and the dynamical fermion mass is substantially enhanced. In particular, we found that the effective fermion mass [$\Delta(0) = 2.15 \times 10^{-6}\Lambda$ for graphene on SiO$_2$ with $\alpha = 0.8$ and $\Delta(0) = 9.62 \times 10^{-6}\Lambda$ for suspended graphene with $\alpha = 2.2$] is much larger than the bare fermion mass ($m = 10^{-7}\Lambda$). Apparently, the enhancement of the fermion mass originates from the excitonic pairing instability due to Coulomb interaction.

When the fermions have small bare mass, an approximate chiral symmetry is dynamically broken, thus there appear massive Goldstone excitons. In the symmetry-breaking phase, there are no massless excitations, and all fermionic and bosonic excitations become massive. We calculated the masses of Goldstone-type excitons using the SVZ sum-rule method developed and widely used in QCD and show that they are larger than bare fermion mass but smaller than dynamical fermionic gap $2\Delta(0)$. In order to take into account the effect of chiral symmetry breaking, the OPE technique was used in the calculation of the two-point correlation functions. In graphene, besides the Goldstone-type exciton, it is also interesting to study the non-Goldstone-type, spin excitons. We specified their positions by the same SVZ sum-rule method and found that the masses of these spin excitons are much larger than bare fermion mass but smaller than $2\Delta(0)$. Moreover, their masses are larger than those of Goldstone-type excitons.

In the theoretical treatment of graphene, the most widely used approximation is to keep only the nearest hopping and expand the fermion energy around the neutral Dirac points. Additional terms will be included in the effective continuous field theory when higher-order corrections are taken into account. Some of these terms may break the chiral symmetry. Generally, the symmetry-breaking terms can appear in two classes: either as quadratic terms $\bar{\psi}\Gamma\psi$ or as quartic terms $(\bar{\psi}\Gamma\psi)^2$ with $\Gamma = 1, \gamma_3, i\gamma_5$. The former corresponds to fermion mass terms and through a unitary transformation of the 4-spinor ψ the coefficients of $\bar{\psi}\Gamma\psi$ can be absorbed into the bare fermions mass m_s introduced in our Eq. (1). Since our calculations and results depend only on the magnitude of m_s, not on its physical origins, such terms will not qualitatively affect our conclusion if they are sufficiently small. The quartic term $(\bar{\psi}\psi)^2$ can be considered as a Hubbard-type short-range interaction term. Its effect is more complex than quadratic terms because we need to study the interplay of the long-range Coulomb interaction and this short-range interaction.[7] When such short-range interaction is weak, its contribution to the Dyson-Schwinger gap equation (3) can be studied by the methods presented in Ref. 7. The calculations of the masses of Goldstone bosons and non-Goldstone bosons can be performed using the sum-rule and OPE methods of Secs. III and IV, because these calculations rely only on the chiral condensate, which is easily obtained from the fermion gap function. However, if this quartic interaction is strong, the whole Lagrangian of the continuous theory is no longer chiral symmetric, and there will not be dynamical chiral symmetry breaking and Goldstone bosons. Indeed, our calculations are based on the assumption that the symmetry-breaking interaction is absent or sufficiently weak.

After obtaining the masses of various types of exciton, the next problem is to judge whether and when these collective modes exist in graphene. Since their masses correspond to the resonance positions in the low-energy region, we hope that NMR and neutron scattering might be able to address this problem, similar to the efforts in high-temperature superconductors.[51–53] To make a connection with experiments, it is also necessary to calculate some observable quantities that can describe the effects of massive excitons. This issue is beyond the scope of the present paper and will be discussed in the future.

*cxzhang.zhang373@gmail.com, cxzhang@nudt.edu.cn
†gzliu@ustc.edu.cn
‡mqhuang@nudt.edu.cn

[1] A. H. Castro Neto, F. Guinea, N. M. R. Peres, K. S. Novoselov, and A. K. Geim, Rev. Mod. Phys. **81**, 109 (2009).

[2] S. Das Sarma, S. Adam, E. H. Hwang, and E. Rossi, e-print arXiv:1003.4731 (to be published).

[3] V. P. Gusynin, S. G. Sharapov, and J. P. Carbotte, Int. J. Mod. Phys. B **21**, 4611 (2007).

[4] S. Das Sarma, E. H. Hwang, and W. K. Tse, Phys. Rev. B **75**, 121406(R) (2007).

[5] D. V. Khveshchenko, Phys. Rev. Lett. **87**, 246802 (2001); D. V. Khveshchenko and H. Leal, Nucl. Phys. B **687**, 323 (2004).

[6] E. V. Gorbar, V. P. Gusynin, V. A. Miransky, and I. A. Shovkovy, Phys. Rev. B **66**, 045108 (2002).

[7] G.-Z. Liu, W. Li, and G. Cheng, Phys. Rev. B **79**, 205429 (2009).

[8] S. Hands and C. Strouthos, Phys. Rev. B **78**, 165423 (2008); W. Armour, S. Hands, and C. Strouthos, *ibid*. **81**, 125105 (2010).

[9] J. E. Drut and T. A. Lahde, Phys. Rev. Lett. **102**, 026802 (2009); Phys. Rev. B **79**, 165425 (2009).

[10] Y. Araki and T. Hatsuda, Phys. Rev. B **82**, 121403(R) (2010); Y. Araki, e-print arXiv:1010.0847 (to be published).

[11] O. V. Gamayun, E. V. Gorbar, and V. P. Gusynin, Phys. Rev. B **81**, 075429 (2010).

[12] D. T. Son, Phys. Rev. B **75**, 235423 (2007).

[13] Y. Nambu and G. Jona-Lasinio, Phys. Rev. **122**, 345 (1961).

[14] C. Chamon, C.-Y. Hou, R. Jackiw, C. Mudry, S.-Y. Pi, and A. P. Schnyder, Phys. Rev. Lett. **100**, 110405 (2008).

[15] C. Y. Hou, C. Chamon, and C. Mudry, Phys. Rev. Lett. **98**, 186809 (2007).

[16] R. Dillenschneider, Phys. Rev. B **78**, 115417 (2008).

[17] C. L. Kane and E. J. Mele, Phys. Rev. Lett. **95**, 226801 (2005).

[18] A. H. Castro Neto, Physics **2**, 30 (2009).

[19] S. Weinberg, *The Quantum Theory of Fields* , Vol. II. (Cambridge University Press, New York, 1996).

[20] K. Wilson, Phys. Rev. **179**, 1499 (1969).

[21] L. P. Kadanoff, Phys. Rev. Lett. **23**, 1430 (1969).

[22] M. Shifman, Prog. Theor. Phys. Suppl. **131**, 1 (1998).

[23] A. M. Tsvelik, *Quantum Field Theory in Condensed Matter Physics* (Cambridge University Press, Cambridge, England, 1995).

[24] M. A. Shifman, A. I. Vainstein, and Z. I. Zakharov, Nucl. Phys. B **147**, 385 (1979).

[25] M. A. Shifman, A. I. Vainstein, and Z. I. Zakharov, Nucl. Phys. B **147**, 448 (1979).

[26] R. Rosenfelder, Z. Phys. C **27**, 496 (1985).

[27] E. Braaten and L. Platter, Phys. Rev. Lett. **100**, 205301 (2008).

[28] D. Gross and A. Neveu, Phys. Rev. D **10**, 3235 (1974).

[29] B. Rosenstein, B. J. Warr, and S. H. Park, Phys. Rep. **205**, 59 (1991).

[30] V. A. Miransky, *Dynamical Symmetry Breaking in Quantum Field Theories* (World Scientific, Singapore, 1993).

[31] C. D. Roberts and A. G. Williams, Prog. Part. Nucl. Phys. **33**, 477 (1994).

[32] T. Appelquist, D. Nash, and L. C. R. Wijewardhana, Phys. Rev. Lett. **60**, 2575 (1988).

[33] T. Appelquist, A. G. Cohen, and M. Schmaltz, Phys. Rev. D **60**, 045003 (1999).

[34] N. Seiberg and E. Witten, Nucl. Phys. B **426**, 19 (1994); **431**, 484 (1994).

[35] T. Appelquist, J. Terning, and L. C. R. Wijewardhana, Phys. Rev. Lett. **75**, 2081 (1995).

[36] A. M. Polyakov, Nucl. Phys. B **120**, 429 (1977).

[37] P. Maris, Phys. Rev. D **52**, 6087 (1995).

[38] P. A. Lee, N. Nagaosa, and X.-G. Wen, Rev. Mod. Phys. **78**, 17 (2006).

[39] S. Ryu, C. Mudry, C. Y. Hou, and C. Chamon, Phys. Rev. B **80**, 205319 (2009).

[40] H. S. Zong, S. Qi, W. Chen, W. M. Sun, and E. G. Zhao, Phys. Lett. B **576**, 289 (2003).

[41] C. J. Burden, Nucl. Phys. B **387**, 419 (1992).

[42] P. Colangelo and A. Khodjamirian, in *At the Frontier of Particle Physics/Handbook of QCD*, edited by M. Shifman (World Scientific, Singapore, 2001).

[43] P. Pascual and R. Tarrach, *QCD: Renormalization For Practitioner* (Springer-Verlag, Berlin, 1984).

[44] M. Shifman, in *At the Frontier of Particle Physics/Handbook of QCD*, edited by M. Shifman (World Scientific, Singapore, 2001).

[45] R. Hofmann, Prog. Part. Nucl. Phys. **52**, 299 (2004).

[46] W. Rantner and X.-G. Wen, Phys. Rev. B **66**, 144501 (2002).

[47] L. Durand, B. Durand, and J. B. Whitenton, Phys. Rev. D **28**, 607 (1983).

[48] G. Baskaran and S. A. Jafari, Phys. Rev. Lett. **89**, 016402 (2002).

[49] S. A. Jafari and G. Baskaran, Eur. Phys. J. B **43**, 175 (2002).

[50] M. Ebrahimkhas, S. A. Jafari, and G. Baskaran, e-print arXiv:0910.1180 (to be published).

[51] B. H. Seradjeh and I. F. Herbut, Phys. Rev. B **76**, 024503 (2007).

[52] A. Ong, G. S. Uhrig, and O. P. Sushkov, Phys.Rev. B **80**, 014514 (2009).

[53] H. Y. Kee and D. Podolsky, Europhys. Lett. **86**, 57005 (2009).